Modeling UWB Multipath Propagation Considering Material-Dependent Reflection Effects

Torben Winkel*, Sven Ole Schmidt† and Horst Hellbrück†
Luebeck University of Applied Sciences, Germany
Department of Electrical Engineering and Computer Science
* Email: torben.winkel@stud.th-luebeck.de
† Email: sven.ole.schmidt, horst.hellbrueck@th-luebeck.de

***Abstract*—In Industry 4.0, indoor localization evolves as an important research area. Ultra-Wide-Band (UWB) transceiver systems allow single-anchor based tag localization. The short temporal extent of UWB signal impulses enables the interpretation of multi-propagation paths. Accordingly, the anchor captures the Channel Impulse Response (CIR) of superposed signal echoes from all existing paths. Reconstruction of superposing effects at the receiver antenna requires the prediction of each path's received signal power. So far, prediction models consider propagation losses. In the case of reflections, the losses of UWB signals are not well documented. Therefore, we introduce a new transceiver model considering multipath and material-depending reflection losses. Based on our measurements, we show the material-dependency of reflection losses and quantify them by refraction indices as we introduce them in our model.**

***Index Terms*—single anchor localization, channel impulse response, ultra-wide-band, multipath propagation, interference, reflection losses, refraction indices, Internet of Things**

I. Introduction

Industrial cost-efficient indoor localization is still an addressed researcher's field. Especially for future applications like Industry 4.0, it becomes important. Today's approaches base on trilateration with multiple anchors for the same area [1]. This approach comes with high installation costs. The upcoming Ultra-Wide-Band (UWB) technology allows precise localization with a single anchor. Due to their wide spectrum, UWB signals have a small temporal resolution. Hence, occurring multipath propagation effects are evaluable. This enables trilateration with a single anchor evaluating the reception of the same signal impulse over several paths. To improve prediction, we introduce a model for multipath propagation considering reflection materials. Therefore, we determine propagation delay and signal power reduction for a known multipath environment. Signal power reduction mainly depends on the propagated distance and reflection losses, which we show are material-dependent.

The contributions of this paper are:

- We develop a transceiver model for UWB multipath propagation
- We investigate material-dependent reflection effects
- We evaluate reflection losses by real measurements for different materials
- We quantify the material-dependency of reflection losses by our transceiver model

First, we give in Section II an overview on indoor localization technologies with UWB signals. In Section III we introduce our transceiver model. Therefore, we investigate the principle of multipath propagation and material-dependent reflection effects. Afterwards, we evaluate our model by real measurements in Section IV. We conclude our paper in Section V and give an outlook on future investigations.

II. Related Work

This section provides an overview related to indoor localization system applying UWB signals. Cimdins et al. introduce a passive localization approach based on a fingerprint matrix [2]. Therefore, the system detects changes in the received signal strength caused by obstacles. Active localization bases on a trilateration of either time of arrival or received signal strength information. Time of arrival systems come with a higher accuracy [3], whereas received signal strength systems require no efforts regarding synchronization of tag and anchor [4]. However, single anchor approaches require fewer installed antennas, thus reducing the installation costs for active and passive localization systems. Giorgetti et al. realize the single anchor by a switched beam antenna with several smaller antennas oriented in different directions [5]. In Großwindhager et al., they employ multipath propagation with the utilization of virtual anchors [6]. In this paper, we introduce a model to predict the received signal strength in a multipath environment for UWB signals. Therefore, we apply the free space equation for propagation losses, as stated in Matthews et al. [7]. We predict the reflection losses by Fresnel's equations as Zhang et al. prove their applicability regarding UWB signals in theory [8]. Accordingly, we measure reflection losses for different materials. The next section announces the aspects of our model in detail.

III. Modeling of Multipath Propagation

Previously we reasoned the necessity for material-dependent reflection loss predictions in indoor localization systems. Referring to this, we introduce a model for UWB multipath propagation in this section. In the first step, we describe the multipath environment with anchor and tag. In the second step, we consider propagation and reflection losses.

A. Multipath Propagation

A single anchor localizes tags in a room. Therefore, tags transmit repeating UWB impulses. In our setup, we transmit on UWB channel 2. The signal has a bandwidth B of 499.2 MHz with a center frequency f_c of 3993.6 MHz. Figure 1 shows the transmitted signal $x(t)$ of UWB channel 2 [9]. These signals propagate wireless in space.

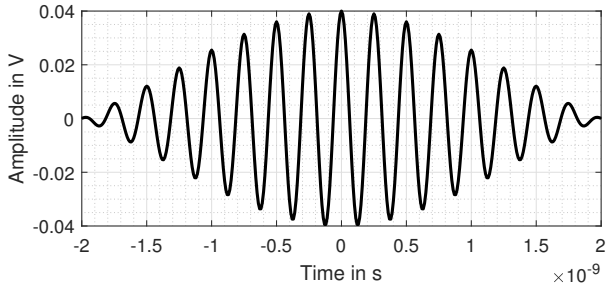

Fig. 1: Reference pulse of UWB channel 2

Reflections occur at interfaces between different mediums, as shown in Figure 2. Hence, the anchor receives each signal impulse several times. At first, it arrives over the direct path, which we name Line of Sight (LOS) path. On the LOS path, no reflections occur. On indirect paths, the Non-Line of Sight (NLOS) paths, at least one obstacle cause signals to reflect. Additionally, they arrive delayed due to longer path lengths.

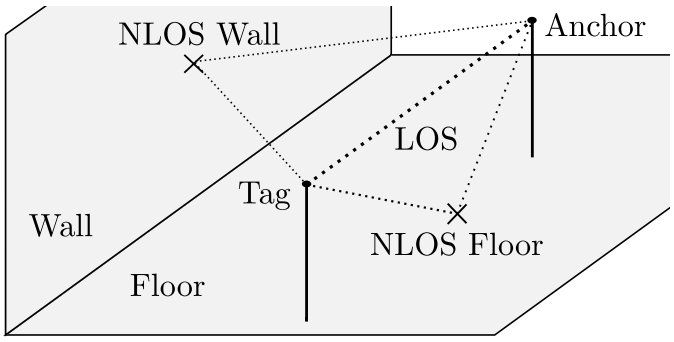

Fig. 2: Common room geometry with floor and wall and multipath signal propagation between tag and anchor

Accordingly, we model the propagation delay of each signal impulse as time-shifted Dirac-function $\delta(t-\tau_i)$. Each impulse i has a magnitude $P_{Rx,i}$ and a timestamp τ_i. A time domain based mathematical model of all received impulses is the Channel Impulse Response (CIR) $h(t)$:

$$h(t) = \sum_{i=0}^{I-1} P_{Rx,i} \cdot \delta(t-\tau_i) \cdot (-1)^{k_i} \tag{1}$$

where $i = 0$ represents the LOS path and $i > 0$ NLOS paths. Each reflection causes a phase shift of π [10]. Therefore, we introduce the factor $(-1)^{k_i}$, where k_i stands for the number of reflections. Figure 3 shows the CIR with Dirac-functions.

Depending on their phases, time-wise overlapping signals superpose in a constructive or nonconstructive way. To model the received signal $y(t)$ we convolve the transmitted signal $x(t)$ and the modeled CIR $h(t)$:

$$y(t) = x(t) * h(t) \tag{2}$$

Figure 3 shows the CIR $h(t)$ and the received signal $y(t)$. In the next subsection, we investigate the received signal power in more detail.

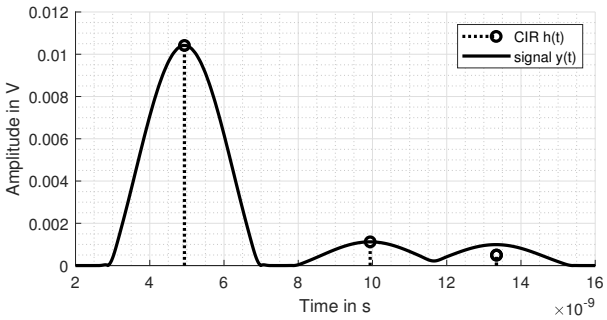

Fig. 3: CIR $h(t)$ and actual received signal $y(t)$ from our model for a common indoor environment; LOS pulse at 5ns and one NLOS pulse at 10ns and another two at 13ns

B. Propagation and Reflection Losses

In the previous subsection, we introduced the multipath environment and the received CIR. In this subsection, we come up with a model to predict the amplitude of received CIRs. Propagation losses P_{PL} and reflection losses P_{RL} reduce the amplitude, where the reflection losses depend on the reflecting material. This leads to a received power amplitude $P_{Rx,i}$ for the i-th path of:

$$P_{Rx,i} = P_{Tx} - P_{PL,i} - P_{RL,i} \tag{3}$$

where P_{Tx} is the transmit power.

In the following, we cover the propagation losses of the transmitted signal. Propagation losses increase with the path's distance d_i:

$$P_{PL,i} = 10 \cdot \gamma \cdot \log_{10} \left| \frac{\lambda}{4\pi d_i} \right| [dB] \tag{4}$$

where γ represents environmental specific propagation losses and λ the wavelength of the signal's carrier frequency f_c.

Interfaces between different materials cause an electromagnetic wave to reflect partly and the rest of it to pass through [10]. Figure 4 shows this behavior. The amount of the reflected power depends on both material's refraction indices. For indoor localization, occurring reflections between air and the material of wall, ceiling and floor are of interest. Accordingly, we define the refraction of air as $n_1 = 1$ and that one of the reflecting material as n_2. The incoming and reflected waves lie on the plane of incidence, which is perpendicular to the reflecting surface. The incoming wave and the normal vector of the reflecting surface enclose the reflection angle α. The reflecting material emits the reflected wave with the same angle α. The incoming wave's electric field consists of an s- and

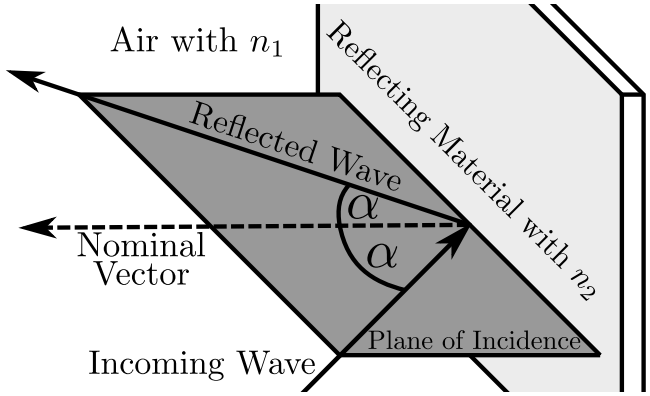

Fig. 4: Occurring reflection at material interface

p-polarized component. The reflection losses depend on the polarization. The s-polarized component is the electric field component normal to the plane of incidence. The p-polarized component consists of the electric field component lying in the plane of incidence. Accordingly, the reflection losses $P_{RL,s}$ and $P_{RL,p}$ of the s- and p-polarized components are [10]:

$$P_{RL,s} = 10\log_{10}\left|\frac{n_1\cos\alpha - \sqrt{n_2^2 - n_1^2\sin^2\alpha}}{n_1\cos\alpha + \sqrt{n_2^2 - n_1^2\sin^2\alpha}}\right|[dB] \quad (5)$$

$$P_{RL,p} = 10\log_{10}\left|\frac{n_2^2\cos\alpha - n_1\sqrt{n_2^2 - n_1^2\sin^2\alpha}}{n_2^2\cos\alpha + n_1\sqrt{n_2^2 - n_1^2\sin^2\alpha}}\right|[dB] \quad (6)$$

Additionally, reflections cause a phase shift of π. In the next section, we measure the CIR and compare it with our modeled one.

IV. Measurement and Evaluation of Multipath Propagation

Previously, we introduced our model. In this section, we come up with a measurement setup. With the help of the setup, we estimate the propagation losses and the path loss exponent. Finally, we evaluate the reflection losses for all materials.

A. Measurement Setup

In this subsection, we introduce our measurement setup to capture the reflection impulses for different materials. Figure 5 shows the positioning of our antennas. Both tag and anchor antennas facing towards each other. The distance d_{LOS} between them is 0.28m. Floor and ceiling reflections do not contain any valuable information for our concerns. This is why we overlap their signals. Hence, the floor distance h_{floor} equals the ceiling distance $h_{ceiling}$, which is 1.40m in our setup. This results in a path length d_{floor} and $d_{ceiling}$ of 2.80m. For our reflection measurements, we introduce different materials in the NLOS wall path. Therefore, we either place our setup in front of a wall, or we introduce an obstacle. The distance between both antennas and wall h_{wall} is 0.88m resulting in a path length d_{wall} of 1.78m.

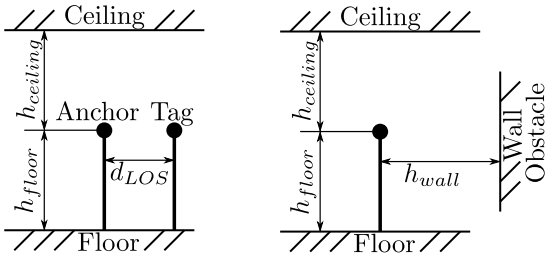

(a) Frontview (b) Sideview

Fig. 5: Setup of our measurements

Our tag as well as our anchor utilize Decawave WB002 antennas [11]. They provide an omnidirectional gain of 2.2 dBi at 4 GHz. The antennas have an impedance of 50 Ω. The emitted waves are vertically polarized. A Tektronix AWG70000a signal generator creates the transmission signal on UWB channel 2 signal (Figure 1). Once generated, an active amplifier gains the signal before transmission by 20dB. A Tektronix DPO70000dx oscilloscope samples the received data from our anchor with 50 GHz. For each setup, we capture the average of over 5000 signal pulses.

Antenna ringing and other multipath propagations superpose with our wall reflection. Because of that, we first capture an idle measurement without introduced obstacles on the wall reflection path. In a second step, we introduce obstacles made of different materials and repeat the measurement. Small inaccuracies occur among single measurements. To make them comparable, we align the time axis and the power level. Afterward, we subtract both idle and material measurements from each other. This leads us to the pure reflection pulse as shown for all materials in Figure 6. In the next subsections, we investigate the propagation and occurring reflection losses.

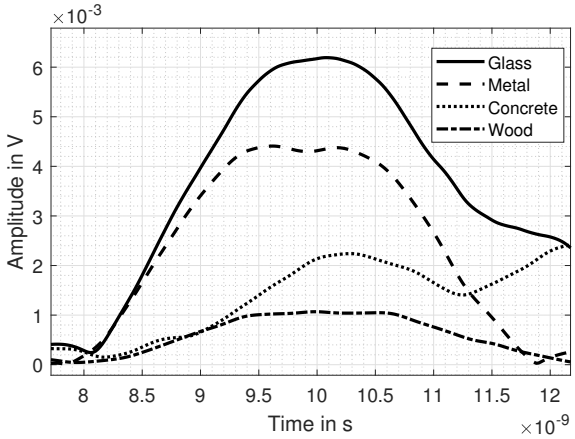

Fig. 6: NLOS wall pulses with reflection at glass, metal, concrete and wood; at 11.4 ns the pulses start to interfere with the NLOS ceiling and floor pulse

B. Propagation Losses

The previous section introduced our measurement setup and how we interpret our received signal pulses. In this subsection,

we evaluate the propagation losses. Therefore, we investigate the LOS pulse of our idle measurements as shown in Figure 7, where the distances d_{LOS} are 0.28m, 0.56m and 1.12m. Hence, we obtain the signal power losses in dependency on the distance. To determine the energy $E_{Rx,i}$ of LOS or NLOS

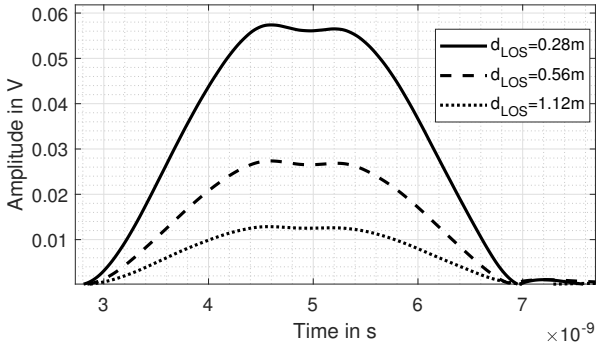

Fig. 7: LOS pulses of our idle measurements for different distances d_{LOS}, where the pulses are time-wise aligned

pulses, we integrate over its duration $t_{d,i}$:

$$E_{Rx,i} = \int^{t_{d,i}} P_{Rx,i}(t) \cdot dt \tag{7}$$

Table I shows the results. The received energies $E_{Rx,1}$ along

TABLE I: Received LOS pulses with varying distances

d_{LOS}	$t_{d,1}$	$E_{Rx,1}$
$0.28m$	$4ns$	$66.08fJ$
$0.56m$	$4ns$	$14.78fJ$
$1.12m$	$4ns$	$3.29fJ$

with the distances d_{LOS} delivers us the path loss exponent γ according to equation 4. Building the average of all LOS path combinations delivers us a path loss exponent of $\gamma = 2.164$. Up next, we calculate the reflection losses.

C. Reflection Losses

In the previous subsection, we determined the path loss exponent γ of our measurement environment. In this section, we investigate the reflection losses. Therefore, we determine the received energy from our reflection pulse of the introduced material. The reflection pulses for different materials are shown in Figure 6. Due to the small path difference, the NLOS wall pulse interferes with the ceiling and floor pulses for 0.6ns. Because of that, we determine each path's received energy over the first 3.4ns. Hence, the LOS pulse energy $E_{Rx,1}$ resulting form the shorter interval is 65.11fJ. Table II shows the energy for all NLOS pulses $E_{Rx,2}$.

The difference between LOS energy $E_{Rx,1}$ and NLOS energy $E_{Rx,2}$ contains propagation losses as well as reflection losses. By subtracting the expected propagation losses on the NLOS wall path $P_{PL,2}$ and adding these one of the LOS path $P_{PL,1}$ we end up with the reflection losses P_{RL}:

$$P_{RL} = 10 \cdot \log_{10} \left| \frac{E_{Rx,1}}{E_{Rx,2}} \right| - P_{PL,2} + P_{PL,1} \tag{8}$$

TABLE II: Energy over 3.4ns of reflection impulses $E_{Rx,2}$, occurring reflection losses P_{RL} and refraction indices n_2 for different materials

Material	$E_{Rx,2}$ (NLOS)	P_{RL}	n_2
Glass	$0.7556fJ$	$-2.0dB$	4.43
Metal	$0.3851fJ$	$-4.9dB$	1.95
Concrete	$0.0934fJ$	$-11.1dB$	1.17
Wood	$0.0226fJ$	$-17.2dB$	1.04

Since our tag emits a vertical polarized wave, the incoming wave reflecting at the wall is purely p-polarized. Hence, we determine the refraction index n_2 via numerical solution based on Equation 5, where the refraction angle α is 9° in our setup. As listed in Table II, we prove the material-dependency of reflection losses and quantify them with refraction indices.

V. Conclusion and Future Work

In this paper, we introduce a model for UWB multipath environments considering propagation and reflection losses. Our measurements expose a better reflectivity of glass and metal compared to concrete and wood. By our model, we determine the refraction indices of these materials. Hence, our model enables the prediction of material-dependent reflection effects for different measurement setups.

In the future, we evaluate the accuracy of our model with different measurement scenarios. Additionally, we apply the results in the context of indoor single anchor localization.

Acknowledgements

This publication results from the research of the Center of Excellence CoSA for the project MOIN (BMWi FKZ ZF4186108BZ8). MOIN is a joint project of Solcon Systemtechnik GmbH and the University of Applied Sciences Lübeck. Horst Hellbrück is an adjunct professor at the Institute of Telematics of the University of Lübeck.

References

[1] F. Zafari, A. Gkelias, and K. K. Leung, "A survey of indoor localization systems and technologies," 2019.
[2] M. Cimdins, S. O. Schmidt, and H. Hellbrück, "Modeling the magnitude and phase of multipath uwb signals for the use in passive localization," 2019.
[3] A. Chaisang and S. Promwong, "Indoor localization distance error analysis with uwb wireless propagation model using positioning method," 2018.
[4] T. Gigl, G. J. Janssen, V. Dizdarević, K. Witrisal, and Z. Irahhauten, "Analysis of a uwb indoor positioning system based on received signal strength," 2007.
[5] G. Giorgetti, A. Cidronali, S. K. S. Gupta, and G. Manes, "Single-ancor indoor localization using a switched-beam antenna," 2009.
[6] B. Großwindhager, M. Rath, J. Kulmer, M. S. Bakr, C. A. Boano, K. Witrisal, and K. Römer, "Salma: Uwb-based single-anchor localization system using multipath assistance," 2018.
[7] B. Matthews, S. O. Schmidt, and H. Hellbrück, "Understanding and prediciton of ultra-wide band channel impulse response measurements."
[8] N.-T. Zhang and J. Meng, "Reflection characteristics analysis of ir-uwb signal," 2008.
[9] Decawave, *DW1000 IEEE802.15.4-2011 UWB Transceiver Datasheet*, 2nd ed., 2015.
[10] M. Bass and V. N. Mahajan, *Handbook of Optics*, 3rd ed. McGraw-Hill, 2010.
[11] Decawave, *WB002 Hardware Build Instruction*, 1st ed., 2014.